Thermal Limit Analysis of Radial AMB by Using Finite Difference Method

Chi Ting YEH, Chung Hsien LIN

Industrial Technology Research Institute, Hsinchu, Taiwan 31040, R.O.C.

itriA30380@itri.org.tw, alowlin@itri.org.tw

Abstract

Load capacity of an active magnetic bearings (AMBs) includes the static load capacity, peak transient load capacity and dynamic load capacity. In this paper, a simulation software, SimRaMB, is proposed to estimate the static load capacity which is constrained by the thermal limit of coils. A finite difference method (FDM) algorithm is adopted for the thermal limit analysis of radial AMB. The thermal limit of an eight poles radial magnetic bearing is simulated by SimRaMB and ANSYS, respectively. A thermal test unit of the radial magnetic bearing was built up in which the temperature distributions are measured by 12 thermal couples. The simulation results showed that the difference of temperature at steady-state between SimRaMB and ANSYS is within $0.8°$C. The experimental result also showed that the difference of temperature between SimRaMB and experiment is within $0.89°$C at lower driving current. However, when the driving current comes to 1.5A and 1.8A, the simulation results of SimRaMB and ANSYS are $8.09°$C and $8.58°$C higher than experimental data, respectively. The reason could be that the present study doesn't take into account the influence of temperature to thermal conductivity of material. In order to improve the simulation result, a table of temperature-dependent thermal conductivity will be included in the future.

Keywords : AMB, thermal limit, static load capacity, finite difference method, graphic user interface

1. Introduction

For the application of AMB system, it is important to firstly define the force envelop of AMB (ISO 14839-1, 2002). The load capacity of an AMB is limited by the peak transient load capacity, static load capacity (thermal limit of coil) and the DC voltage limit. For peak transient load capacity and thermal limit analysis of AMB, one could get good simulation results by using several commercial software based on the finite element modeling method. However, the software is very expensive and it always consumes a lot of time for the mechanical component modeling, analysis environmental setting, finite elements meshing and final results calculation.

For industrial application, it is prefer to use the simplified simulation software (Burder, et al., 2004; Ueyama and Taniguchi, 2010) to simulate the preliminary results of AMBs. It can easily input the design data of AMB, such as the mechanical dimensions of magnetic bearing, selection of different kind of silicon steel sheets, copper wire and bobbin size, driving currents, and so on. The software can quickly show up the AMB appearances, electrical properties, magnetic flux along the magnetic loop of bearing, bearing force vs. driving current, and etc. One can further modify the input data to approach the best design according to the result comparison between each simulation. Once the preliminary design of AMB is decided, the critical design can be implemented again by using the commercial software in order to make sure that the requirements of AMB has been satisfactorily met.

In this paper, a simplified simulation software of radial AMB, SimRaMB, is proposed. SimRaMB is developed with MATLAB computer language. It contents the analysis capabilities of both peak transient and static load capacity. Since the transient load design approaches of magnetic bearings have been discussed in many papers, here we will only introduce the thermal limit analysis of SimRaMB which uses the three-dimensional finite difference method (FDM). The radial AMB is meshed and divided into many small cells along the redial, axial and periphery direction. The thermal property of each cell is defined according to its thermal property of material. An algorithm is also designed to define the thermal property of cells which are located at the boundary between different materials, such as silicon steel, bobbin,

copper wire, air and epoxy. The case study for different dimension redial AMBs will be discussed and compared with the simulation results of commercial software. The simulation and experimental results of a radial AMB unit which was used for a liquid pump will be presented as well.

2. Simulator of radial magnetic bearing, SimRaMB

SimRaMB possesses several functions for the radial magnetic bearing design. SimRaMB has a graphic user interface, as shown in Fig. 1, to input the design data of bearing and simulate the results quickly. One can select the type of silicon steel sheets and copper wires from its database. After input of the geometry of bearing, the geometric appearance of bearing will be automatically showed up. Then the user can input the driving current condition. SimRaMB will calculate and show up the figures of the magnetic flux along the bearing loop and force vs. current respectively. The user can modify the design input and compare with previous simulations until the design is satisfied.
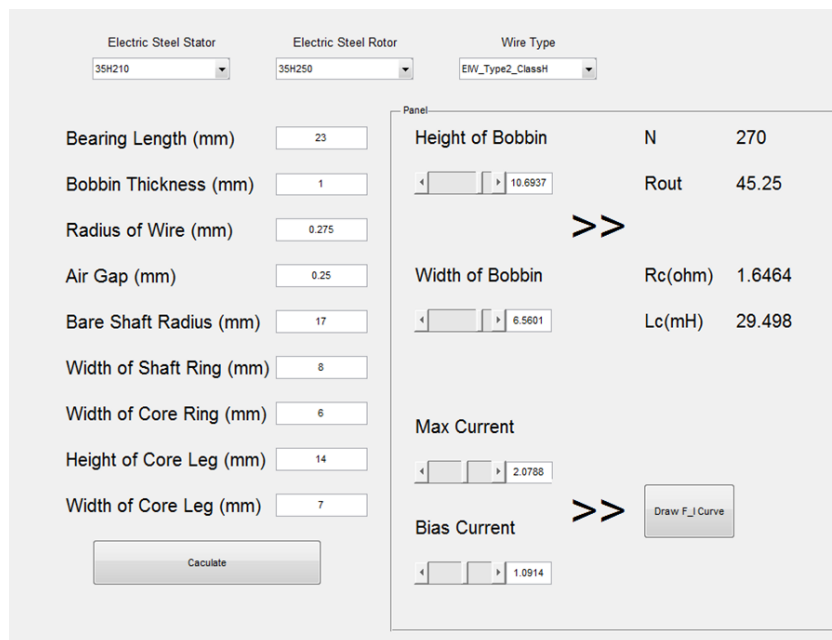

Fig. 1 Graphical User Interface of SimRaMB

The second important function of SimRaMB is "MeshViewer". The MeshViewer can show up the mesh results with different colors for different materials of cell, as shown in Fig. 2. One can check the meshes of radial bearing and change the cell size at either radial and periphery directions until the bearing is properly meshed. The third function of SimRaMB is the calculation of thermal balance of each cell of magnetic bearing which will be presented in the following sections.
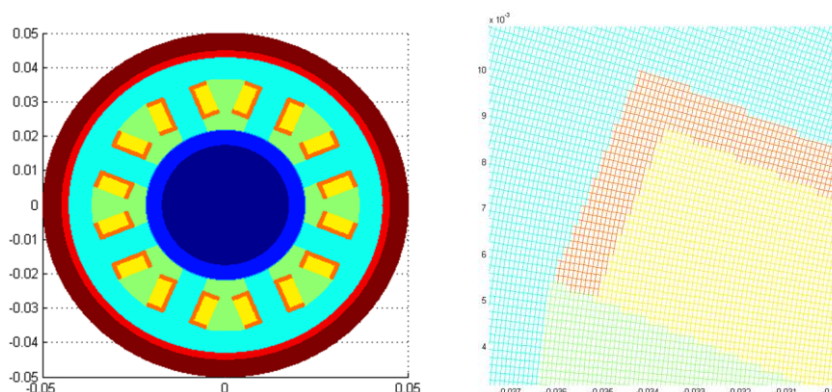

Fig. 2 Mesh results from MeshViewer

3. Energy Balance Method

In this paper, the energy balance method (Incropera, et al., 2007) is adopted to derive the finite difference equations for radial AMB. Assume an arbitrary cell in Fig. 2 as the (m, n) nodal point of radial bearing. If the cell is not exposed to convective condition, the control volume of the (m, n) node is defined as shown in Fig. 3. The heat transfer rates between the (m, n) node and it vicinity nodes are defined as q_1, q_2, q_3, and q_4. According to the energy conservation, the energy exchange of nodes (into or out of the node) can be described as,

$$q_1 + q_2 + q_3 + q_4 + \dot{q}\, r_m\, \Delta r\, \Delta \theta = 0 \tag{1}$$

where r_m is the radius of the (m, n) node. Δr and $\Delta \theta$ are the radial and angular spacing of the control volume of the nodes. $\dot{q}$ is heat generation rate per unit volume caused by energy loss. Considering the temperature and thermal resistance between nodal points, the heat flow terms of (m, n) node can be expressed as:

$$q_1 = (T_{m+1,\,n} - T_{m,\,n})/(\frac{0.5\Delta r}{k_{m+1,\,n}\,\Delta\theta\,(r_m + 0.75\Delta r)} + \frac{0.5\Delta r}{k_{m,\,n}\,\Delta\theta\,(r_m + 0.25\Delta r)}) \tag{2}$$

$$q_2 = (T_{m-1,\,n} - T_{m,\,n})/(\frac{0.5\Delta r}{k_{m-1,\,n}\,\Delta\theta\,(r_m + 0.75\Delta r)} + \frac{0.5\Delta r}{k_{m,\,n}\,\Delta\theta\,(r_m + 0.25\Delta r)}) \tag{3}$$

$$q_3 = (T_{m,\,n-1} - T_{m,\,n})/(\frac{0.5\,\Delta\theta\,r_m}{k_{m,\,n-1}\,\Delta r} + \frac{0.5\,\Delta\theta\,r_m}{k_{m,\,n}\,\Delta r}) \tag{4}$$

$$q_4 = (T_{m,\,n+1} - T_{m,\,n})/(\frac{0.5\,\Delta\theta\,r_m}{k_{m,\,n+1}\,\Delta r} + \frac{0.5\,\Delta\theta\,r_m}{k_{m,\,n}\,\Delta r}) \tag{5}$$

where $T_{m,\,n}$ is the temperature of nodal points and $k_{m,\,n}$ is effective thermal conductivity.
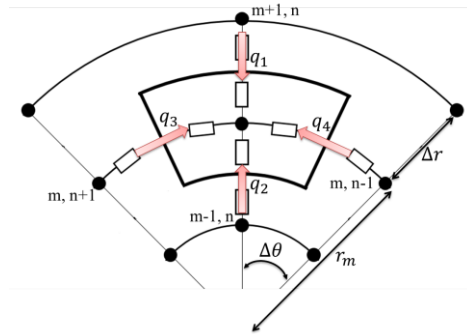

Fig. 3 Nodal network in a 2D cylindrical configuration without convectional cooling

If the cell is exposed to convective condition, such as a cooling system, the control volume of the (m, n) node can be shown in Fig. 4. According to the energy conservation, the energy exchange of nodes can be described as,

$$q_{cooling} + q_2 + q_3 + q_4 + \frac{\dot{q}\,(r_m - \Delta r/4)\,\Delta r\,\Delta \theta}{2} = 0 \tag{6}$$

where $q_{cooling}$ is total convection rate. The heat flow terms of the node with convectional cooling can be expressed as:

$$q_{cooling} = h\,r_m\,\Delta\theta\,(T_\infty - T_{m,\,n}) \tag{7}$$

$$q_2 = (T_{m-1,\,n} - T_{m,\,n})/(\frac{0.5\Delta r}{k_{m-1,\,n}\,\Delta\theta\,(r_m + 0.75\Delta r)} + \frac{0.5\Delta r}{k_{m,\,n}\,\Delta\theta\,(r_m + 0.25\Delta r)}) \tag{8}$$

$$q_3 = (T_{m,\,n-1} - T_{m,\,n})/(\frac{0.5\,\Delta\theta\,(r_m - \Delta r/4)}{k_{m,\,n-1}\,\Delta r/2} + \frac{0.5\,\Delta\theta\,(r_m - \Delta r/4)}{k_{m,\,n}\,\Delta r/2}) \tag{9}$$

$$q_4 = (T_{m,\,n+1} - T_{m,\,n})/(\frac{0.5\,\Delta\theta\,(r_m - \Delta r/4)}{k_{m,\,n+1}\,\Delta r/2} + \frac{0.5\,\Delta\theta\,(r_m - \Delta r/4)}{k_{m,\,n}\,\Delta r/2}) \tag{10}$$

The convection heat transfer coefficient, h coefficient, and the cooling temperature T_∞ express the capacity of the cooling system. Typical values of the convection heat transfer coefficient are listed in Table 1.
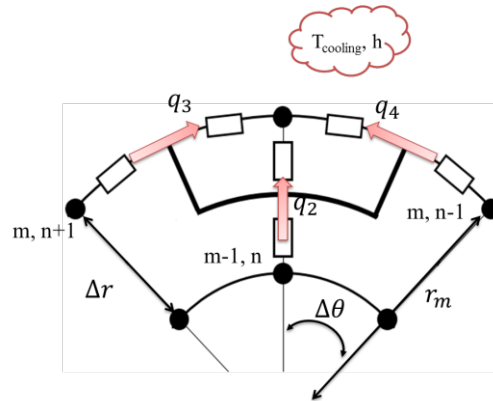
Fig. 4 Nodal network in a 2D cylindrical configuration with convectional cooling

Table 1 Typical values of the convection heat transfer coefficient (Incropera, et al., 2007)

Process	h ($W / m^2 \cdot K$)
Gases Free convection	2-25
Liquids Free convection	50-1000
Gases Forced convection	25-250
Liquids Forced convection	100-20000
Convection with phase change	2500-100000

4. Thermal simulation and Test of Radial Bearing

In order to verify the simulation accuracy of SimRaMB, an eight poles heterpolar radial bearing stator is used for the thermal simulation and experiment. This radial bearing has been used for a liquid regenerative pump, as shown in Fig. 5, which is developed jointly by ITRI, Lightwing Co. and MUTECS. The dimension and geometry of the radial bearing stator are shown in Table 2 and Fig. 6, respectively. The thermal balance of the radial bearing unit was tested to measure the temperature distributions, as shown in Fig. 7. The test unit of radial bearing consists of magnetic cores of silicon steel sheets, copper coils, winding bobbins and bearing casing made by A6061 aluminum. There are 12 thermal couples installed on the coils and magnetic cores for temperature measurement. The thermal conductivity of materials for each bearing components are shown in table 3, in which the thermal conductivity of the bobbin is measured by a thermal constants analyzer (Hot Disk TPS 2500).

Fig. 5 Liquid regenerative pump

Table 2 Dimensions of thermal test unit

Dimension	Parameter	Dimension	Parameter
Outer diameter of casing (Dc)	180 mm	Height of magnetic pole (Hp)	20.85 mm
Outer diameter of stator core (Do)	120 mm	Width of magnetic pole (Wp)	14 mm
Inner diameter of stator core (Di)	60 mm	Height of bobbin (Hb)	14 mm
Casing length	50 mm	Width of bobbin (Wb)	6.4 mm
Bearing length	21 mm	Thickness of bobbin (tb)	2 mm
Wire diameter	0.45 mm	Width of core back ring (Wr)	9.25 mm
Number of coil turns / pole	133		
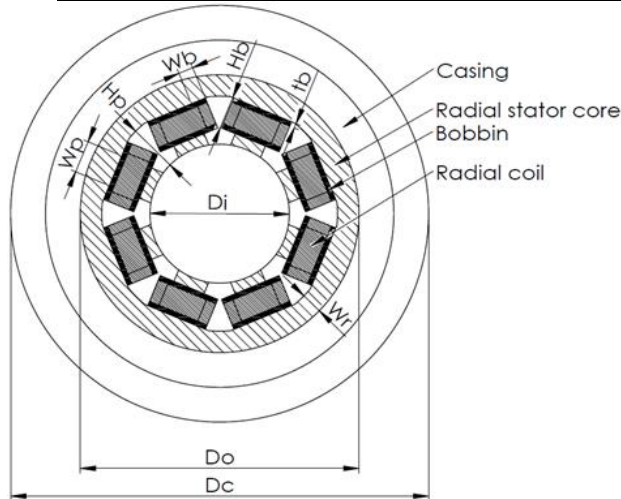
Fig. 6 Geometry sketch of eight-pole radial AMB
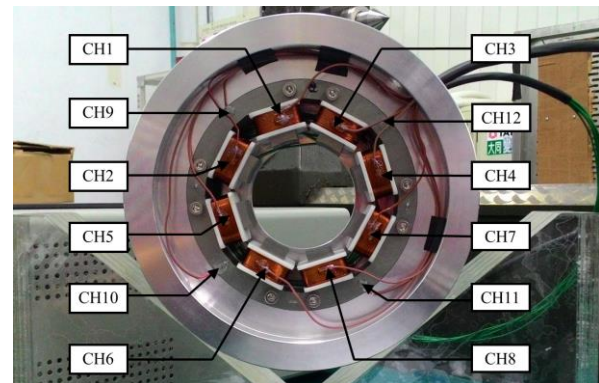
Fig. 7 Thermal test unit of eight-pole radial AMB

Table 3 Thermal conductivity of materials

Material	Thermal Conductivity (W/mK)
Aluminum alloy 6061	155
Copper coil	400
Magnetic core (radial direction)	28 (Gieras, J. F., 2008)
Magnetic core (axial direction)	0.37 (Gieras, J. F., 2008)
Bobbin	0.21

5. Simulation and Experimental Results

The thermal model of present test unit is developed by SimRaMB and MeshViewer. Fig. 8 shows the simulation results of temperature distributions at steady-state. The average temperature of cooling air is assumed as $23.6℃$. For worst-case analysis, we set the four upper coils with maximum driving current by 1A. Figs. 8 and 9 illustrate the results simulated by SimRaMB and ANSYS, respectively. Comparing Figs. 8 and 9, it is obviously that the simulation results between SimRaMB and ANSYS are almost the same.

Fig. 10 shows the experimental results with the same driving conditions of magnetic bearing in Figs. 8 and 9. The temperature measured by the thermal couples (CH1 to CH12) from transient to steady are shown in Fig. 10(a) to Fig. 10(f), respectively. In each figure, the simulation results of SimRaMB and ANSYS are shown as well. As shown in Figs. 10, the simulation result of SimRaMB is very close to that of ANSYS and experiment. The difference of temperature between the experimental and simulation results of SimRaMB is within 0.89°C. The difference of temperature between the simulations of SimRaMB and ANSYS is within 0.8°C.
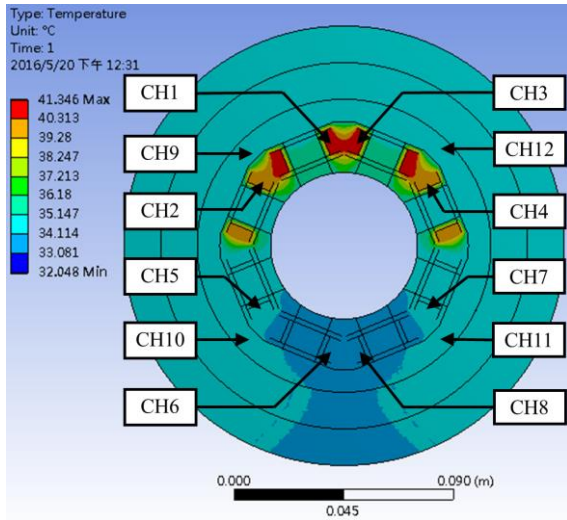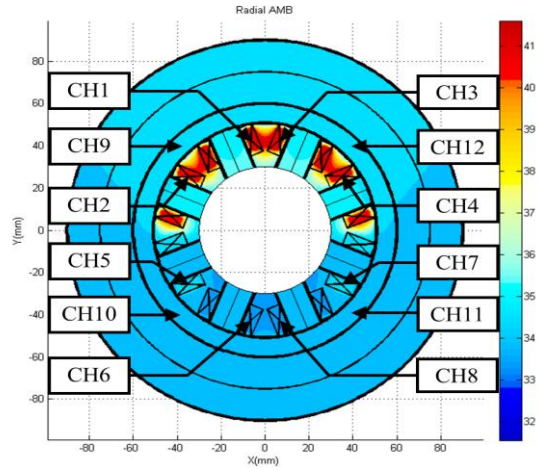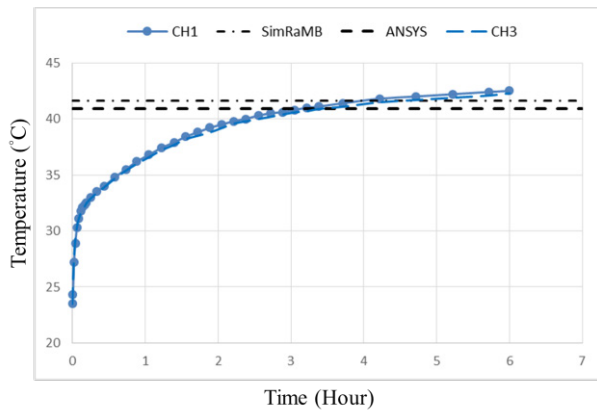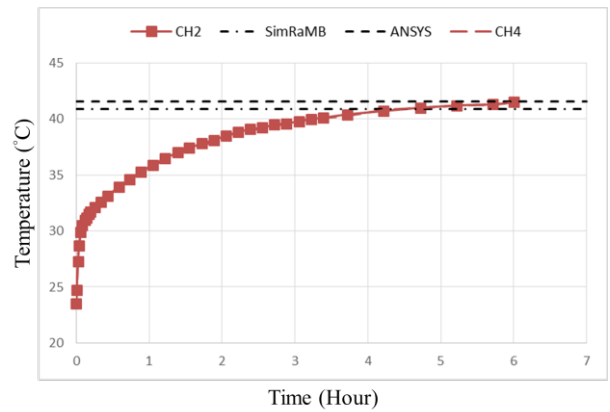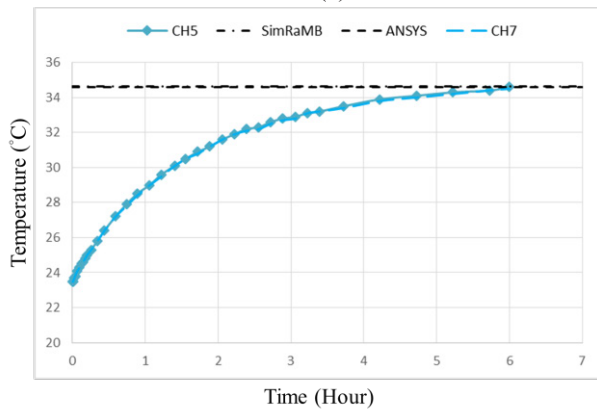
Fig. 8 Simulation result from SimRaMB

Fig. 9 Simulation result from ANSYS

(a)

(b)

(c)
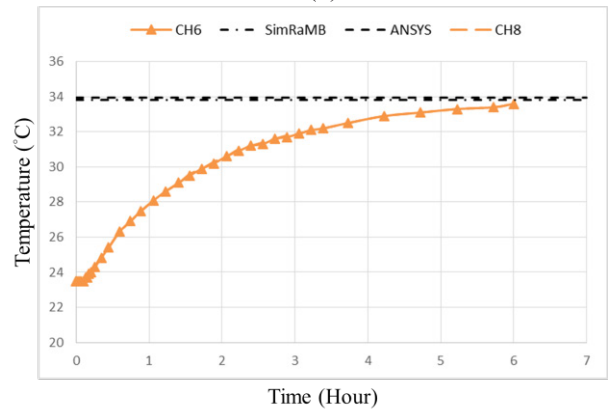

(d)

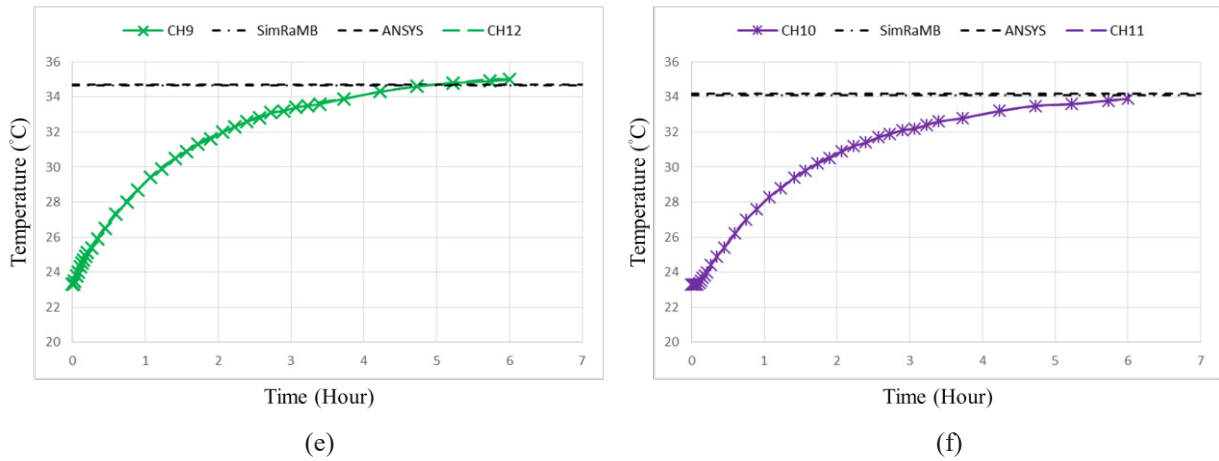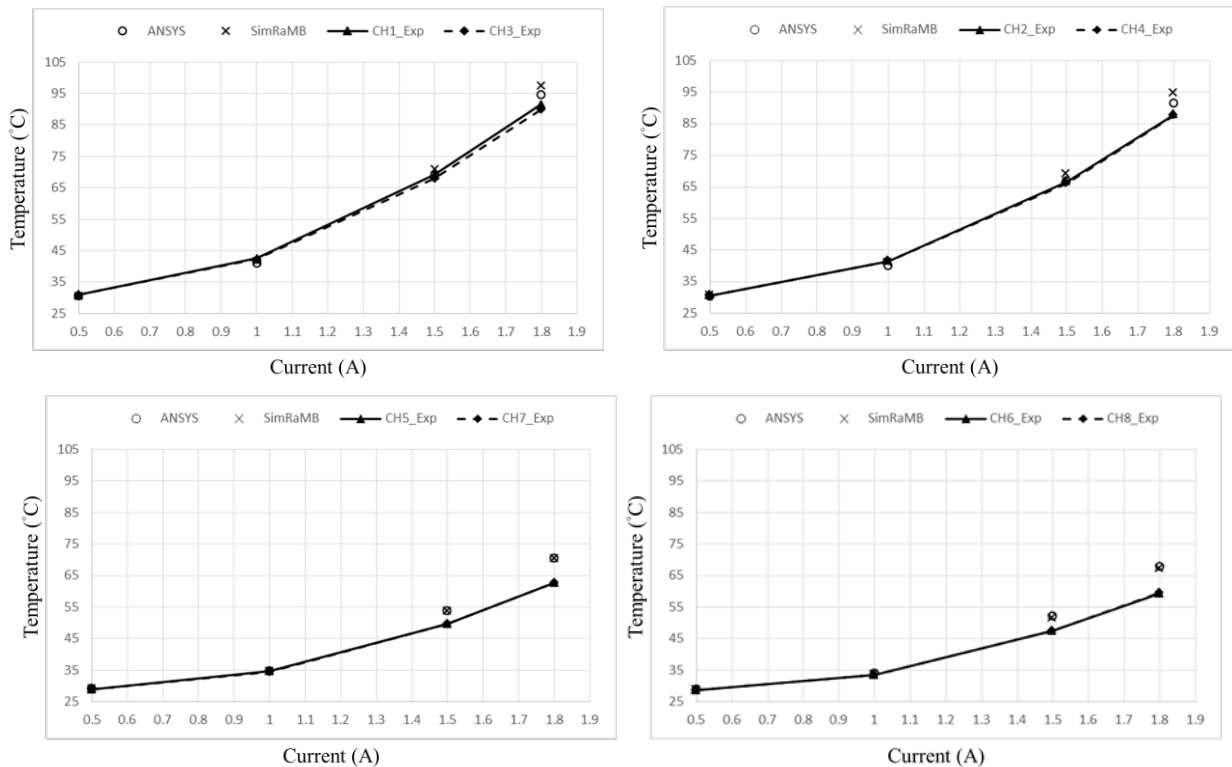<div align="center">(e)   (f)</div>

Fig. 10 Comparison between the measured temperature and simulation results with 1A driving current

Fig. 11 shows the experimental and simulation results of SimRaMB and ANSYS with different driving currents. As shown in Fig. 11, the difference of temperature with 0.5A and 1A driving currents between the simulation and experimental results is within 1.62°C. However, when the driving current comes to 1.5A and 1.8A, the simulation results of SimRaMB and ANSYS are 8.09°C and 8.58°C higher than experimental data, respectively. The higher driving current applied, the higher temperature of simulation will be. In practical, the thermal conductivity of material varies with material temperature. In present paper, the thermal conductivity is assumed to be a constant. It could be the reason that the deviation of temperature between simulation and experiment is getting larger as the temperature increasing. In order to improve the accuracy of simulation result, it shall take into account the influence of temperature to thermal conductivity of material.
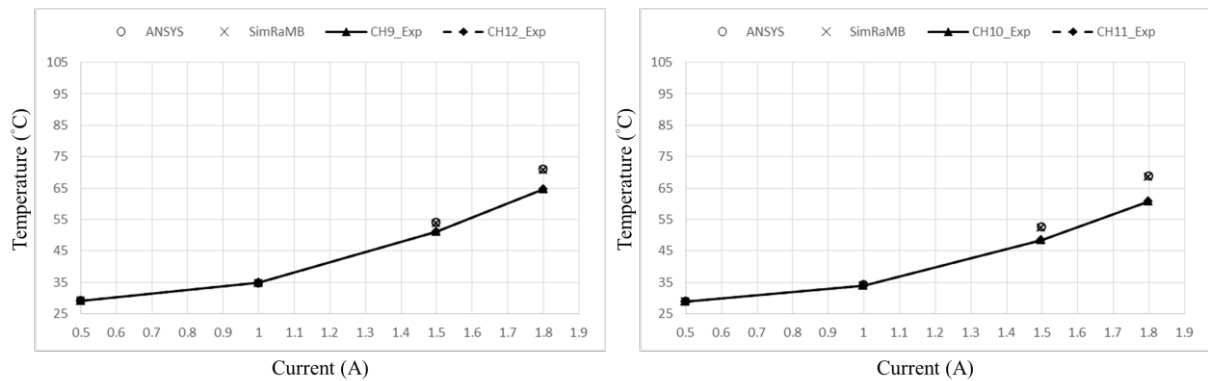
Fig. 11 Comparison between the measured temperature and simulation results

6. Conclusions

This paper presented a thermal simulation tool for design of radial AMBs. The thermal analysis tool comprises two main functions: MeshViewer and FDM algorithm. Thermal model equations used in the FDM algorithm was presented as well. To verify the accuracy of SimRaMB, a thermal test unit was built up in which the temperature distributions are measured by 12 thermal couples. The simulation is implemented by SimRaMB and ANSYS. The results showed that the difference of temperature is within $0.8°C$ at steady-state. The experimental result also showed that the difference of temperature between SimRaMB and experiment is within $0.89°C$ at lower driving current, 0.5A and 1A. Once the driving current increased to 1.5A and 1.8A, the difference of temperature between simulation and experiment increased to $8.09°C$ and $8.58°C$. The reason could be that the present study doesn't take into account the influence of temperature to thermal conductivity of material. In order to improve the simulation result, a table of temperature-dependent thermal conductivity of material will be included in the future.

References

ISO 14839-1, Mechanical vibration - Vibration of rotating machinery equipped with active magnetic bearings - Part 1: Vocabulary, 2002.

Burder, L., Aeschlimann, B. and Siegwart, R., Thermal Model for a High Temperature Active Magnetic Bearing, 9th International Symposium on Magnetic bearing, 2004.

Ueyama, H. and Taniguchi, M., Thermal Simulation of Rotating Machine Equipped with Active Magnetic Bearings, 12th International Symposium on Magnetic bearings, 2010.

Incropera, F.P., DeWitt, D.P., Bergman, T.L. and Lavine, A.S., Introduction to Heat Transfer (5E.), Wiley, New York (2007) pp. 215-217.

Gieras, J. F., Advancements in Electric Machines, Springer Netherlands (2008) pp. 29.